Search for scalar quarks in Z^0 decays

DELPHI Collaboration

P. Abreu [a], W. Adam [b], F. Adami [c], T. Adye [d], G.D. Alexeev [e], J.V. Allaby [f], P. Allen [g],
S. Almehed [h], F. Alted [g], S.J. Alvsvaag [i], U. Amaldi [f], E. Anassontzis [j], W.-D. Apel [k],
B. Asman [ℓ], C. Astor Ferreres [m], J.-E. Augustin [n], A. Augustinus [f], P. Baillon [f], P. Bambade [n],
F. Barao [a], G. Barbiellini [o], D.Y. Bardin [e], A. Baroncelli [p], O. Barring [h], W. Bartl [b], M.J. Bates [q],
M. Baubillier [r], K.-H. Becks [s], C.J. Beeston [q], P. Beilliere [t], I. Belokopytov [u], P. Beltran [v],
D. Benedic [w], J.M. Benlloch [g], M. Berggren [ℓ], D. Bertrand [x], S. Biagi [y], F. Bianchi [z],
J.H. Bibby [q], M.S. Bilenky [e], P. Billoir [r], J. Bjarne [h], D. Bloch [w], P.N. Bogolubov [e], D. Bollini [α],
T. Bolognese [c], M. Bonapart [β], P.S.L. Booth [y], M. Boratav [r], P. Borgeaud [c], H. Borner [q],
C. Bosio [p], O. Botner [γ], B. Bouquet [n], M. Bozzo [δ], S. Braibant [f], P. Branchini [p], K.D. Brand [s],
R.A. Brenner [ε], C. Bricman [x], R.C.A. Brown [f], N. Brummer [β], J.-M. Brunet [t], L. Bugge [ζ],
T. Buran [ζ], H. Burmeister [f], C. Buttar [q], J.A.M.A. Buytaert [x], M. Caccia [n], M. Calvi [n],
A.J. Camacho Rozas [m], J.-E. Campagne [f], A. Campion [y], T. Camporesi [f], V. Canale [p], F. Cao [x],
L. Carroll [y], C. Caso [δ], E. Castelli [o], M.V. Castillo Gimenez [g], A. Cattai [f], F.R. Cavallo [α],
L. Cerrito [p], P. Charpentier [f], P. Checchia [θ], G.A. Chelkov [e], L. Chevalier [c], P. Chliapnikov [u],
V. Chorowicz [r], R. Cirio [z], M.P. Clara [z], J.L. Contreras [g], R. Contri [δ], G. Cosme [n], F. Couchot [n],
H.B. Crawley [κ], D. Crennell [d], M. Cresti [θ], G. Crosetti [δ], N. Crosland [q], M. Crozon [t],
J. Cuevas Maestro [m], S. Czellar [ε], S. Dagoret [n], E. Dahl-Jensen [λ], B. Dalmagne [n], M. Dam [f],
G. Damgaard [λ], G. Darbo [δ], E. Daubie [x], M. Davenport [f], P. David [r], A. De Angelis [o],
M. De Beer [c], H. De Boeck [x], W. De Boer [k], C. De Clercq [x], M.D.M. De Fez Laso [g],
N. De Groot [β], C. De La Vaissiere [r], B. De Lotto [o], A. De Min [n], C. Defoix [t], D. Delikaris [f],
P. Delpierre [t], N. Demaria [z], L.Di Ciaccio [p], A.N. Diddens [β], H. Dijkstra [f], F. Djama [w],
J. Dolbeau [t], K. Doroba [μ], M. Dracos [w], J. Drees [s], M. Dris [ξ], W. Dulinski [w], R. Dzhelyadin [u],
D.N. Edwards [y], L.-O. Eek [γ], P.A.-M. Eerola [ε], T. Ekelof [γ], G. Ekspong [ℓ], J.-P. Engel [w],
V. Falaleev [u], A. Fenyuk [u], M. Fernandez Alonso [m], A. Ferrer [g], S. Ferroni [δ], T.A. Filippas [ξ],
A. Firestone [κ], H. Foeth [f], E. Fokitis [ξ], F. Fontanelli [δ], H. Forsbach [s], B. Franek [d],
K.E. Fransson [γ], P. Frenkiel [t], D.C. Fries [k], R. Fruhwirth [b], F. Fulda-Quenzer [n], H. Furstenau [k],
J. Fuster [f], J.M. Gago [a], G. Galeazzi [θ], D. Gamba [z], U. Gasparini [θ], P. Gavillet [f], S. Gawne [y],
E.N. Gazis [ξ], P. Giacomelli [α], K.-W. Glitza [s], R. Gokieli [r], V.M. Golovatyuk [e], A. Goobar [ℓ],
G. Gopal [d], M. Gorski [μ], V. Gracco [δ], A. Grant [f], F. Grard [x], E. Graziani [p], M.-H. Gros [n],
G. Grosdidier [n], B. Grossetete [r], S. Gumenyuk [u], J. Guy [d], F. Hahn [s], M. Hahn [k], S. Haider [f],
Z. Hajduk [β], A. Hakansson [h], A. Hallgren [γ], K. Hamacher [s], G. Hamel De Monchenault [c],
F.J. Harris [q], B. Heck [f], I. Herbst [s], J.J. Hernandez [g], P. Herquet [x], H. Herr [f], E. Higon [g],
H.J. Hilke [f], T. Hofmokl [μ], R. Holmes [κ], S.-O. Holmgren [ℓ], J.E. Hooper [λ], M. Houlden [y],
J. Hrubec [b], P.O. Hulth [ℓ], K. Hultqvist [ℓ], D. Husson [w], B.D. Hyams [f], P. Ioannou [j],
P.-S. Iversen [i], J.N. Jackson [y], P. Jalocha [π], G. Jarlskog [h], P. Jarry [c], B. Jean-Marie [n],
E.K. Johansson [ℓ], M. Jonker [f], L. Jonsson [h], P. Juillot [w], R.B. Kadyrov [e], G. Kalkanis [j],
G. Kalmus [d], G. Kantardjian [f], F. Kapusta [r], P. Kapusta [π], S. Katsanevas [j], E.C. Katsoufis [ξ],
R. Keranen [ε], J. Kesteman [x], B.A. Khomenko [e], B. King [y], N.J. Kjaer [λ], H. Klein [f], W. Klempt [f],
A. Klovning [i], P. Kluit [x], J.H. Koehne [k], B. Koene [β], P. Kokkinias [v], M. Kopf [k], M. Koratzinos [f],
K. Korcyl [π], A.V. Korytov [e], B. Korzen [f], C. Kourkoumelis [j], T. Kreuzberger [b], J. Krolikowski [μ],

U. Kruener-Marquis [s], W. Krupinski [π], W. Kucewicz [η], K. Kurvinen [ε], M.I. Laakso [ε],
C. Lambropoulos [ν], J.W. Lamsa [κ], L. Lanceri [o], V. Lapin [u], J.-P. Laugier [c], R. Lauhakangas [ε],
P. Laurikainen [ε], G. Leder [b], F. Ledroit [t], J. Lemonne [x], G. Lenzen [s], V. Lepeltier [n],
A. Letessier-Selvon [r], E. Lieb [s], E. Lillestol [f], E. Lillethun [i], J. Lindgren [ε], I. Lippi [θ], R. Llosa [g],
B. Loerstad [h], M. Lokajicek [e], J.G. Loken [q], M.A. Lopez Aguera [m], A. Lopez-Fernandez [n],
D. Loukas [ν], J.J. Lozano [g], R. Lucock [d], B. Lund-Jensen [γ], P. Lutz [t], L. Lyons [q], G. Maehlum [f],
J. Maillard [t], A. Maltezos [ν], F. Mandl [b], J. Marco [m], J.-C. Marin [f], A. Markou [ν], L. Mathis [t],
C. Matteuzzi [η], G. Matthiae [p], M. Mazzucato [θ], M. McCubbin [γ], R. McKay [κ], E. Menichetti [z],
C. Meroni [η], W.T. Meyer [κ], W.A. Mitaroff [b], G.V. Mitselmakher [e], U. Mjoernmark [h], T. Moa [ℓ],
R. Moeller [λ], K. Moenig [s], M.R. Monge [δ], P. Morettini [δ], H. Mueller [k], H. Muller [f], G. Myatt [q],
F. Naraghi [r], U. Nau-Korzen [s], F.L. Navarria [α], P. Negri [η], B.S. Nielsen [λ], V. Nikolaenko [u],
V. Obraztsov [u], R. Orava [ε], A. Ouraou [c], R. Pain [r], H. Palka [π], T. Papadopoulou [ξ], L. Pape [f],
P. Pasini [α], A. Passeri [p], M. Pegoraro [θ], V. Perevozchikov [u], M. Pernicka [b], M. Pimenta [a],
O. Pingot [x], C. Pinori [θ], A. Pinsent [q], M.E. Pol [a], B. Poliakov [u], G. Polok [π], P. Poropat [o],
P. Privitera [α], A. Pullia [η], J. Pyyhtia [ε], A.A. Rademakers [β], D. Radojicic [q], S. Ragazzi [η],
W.H. Range [γ], P.N. Ratoff [q], A.L. Read [ξ], N.G. Redaelli [η], M. Regler [b], D. Reid [γ],
P.B. Renton [q], L.K. Resvanis [j], F. Richard [n], J. Ridky [e], G. Rinaudo [z], I. Roditi [f], A. Romero [z],
P. Ronchese [θ], E.I. Rosenberg [κ], U. Rossi [α], E. Rosso [f], P. Roudeau [n], T. Rovelli [α],
V. Ruhlmann [c], A. Ruiz [m], H. Saarikko [ε], Y. Sacquin [c], E. Sanchez [g], J. Sanchez [g], E. Sanchis [g],
M. Sannino [δ], M. Schaeffer [w], H. Schneider [k], F. Scuri [o], A. Sebastia [g], A.M. Segar [q],
R. Sekulin [d], M. Sessa [o], G. Sette [δ], R. Seufert [k], R.C. Shellard [f], P. Siegrist [c], S. Simonetti [δ],
F. Simonetto [θ], A.N. Sissakian [e], T.B. Skaali [ξ], J. Skeens [κ], G. Skjevling [ξ], G. Smadja [c],
N.E. Smirnov [u], G.R. Smith [d], R. Sosnowski [μ], K. Spang [λ], T. Spassoff [e], E. Spiriti [p],
S. Squarcia [δ], H. Staeck [s], C. Stanescu [p], G. Stavropoulos [ν], F. Stichelbaut [x], A. Stocchi [η],
J. Strauss [b], R. Strub [w], C.J. Stubenrauch [f], M. Szczekowski [μ], M. Szeptycka [μ], P. Szymanski [μ],
S. Tavernier [x], G. Theodosiou [ν], A. Tilquin [t], J. Timmermans [β], V.G. Timofeev [e],
L.G. Tkatchev [e], D.Z. Toet [β], A.K. Topphol [i], L. Tortora [p], D. Treille [f], U. Trevisan [δ],
G. Tristram [t], C. Troncon [η], E.N. Tsyganov [e], M. Turala [π], R. Turchetta [w], M.-L. Turluer [c],
T. Tuuva [ε], I.A. Tyapkin [e], M. Tyndel [d], S. Tzamarias [f], F. Udo [β], S. Ueberschaer [s],
V.A. Uvarov [u], G. Valenti [α], E. Vallazza [z], J.A. Valls Ferrer [g], G.W. Van Apeldoorn [β],
P. Van Dam [β], W.K. Van Doninck [x], N. Van Eijndhoven [f], C. Vander Velde [x], J. Varela [a],
P. Vaz [a], G. Vegni [η], M.E. Veitch [q], J. Velasco [g], L. Ventura [θ], W. Venus [d], F. Verbeure [x],
L.S. Vertogradov [e], L. Vibert [r], D. Vilanova [c], N.K. Vishnevskiy [u], E.V. Vlasov [u],
A.S. Vodopyanov [ς], M. Vollmer [s], G. Voulgaris [j], M. Voutilainen [ε], V. Vrba [e], H. Wahlen [s],
C. Walck [ℓ], F. Waldner [o], M. Wayne [κ], P. Weilhammer [f], J. Werner [s], A.M. Wetherell [f],
J.H. Wickens [x], J. Wikne [ξ], W.S.C. Williams [q], M. Winter [w], D. Wormald [ξ], G. Wormser [n],
K. Woschnagg [γ], N. Yamdagni [ℓ], P. Yepes [β], A. Zaitsev [u], A. Zalewska [π], P. Zalewski [μ],
P.I. Zarubin [e], E. Zevgolatakos [ν], G. Zhang [s], N.I. Zimin [e], R. Zitoun [r],
R. Zukanovich Funchal [t], G. Zumerle [θ] and J. Zuniga [g]

[a] *LIP, Av. Elias Garcia 14 - 1e, P-1000 Lisbon Codex, Portugal*

[b] *Institut für Hochenergiephysik, Österreichische Akademie der Wissenschaften, Nikolsdorfergasse 18, A-1050 Vienna, Austria*

[c] *DPhPE, CEN-Saclay, F-91191 Gif-Sur-Yvette Cedex, France*

[d] *Rutherford Appleton Laboratory, Chilton, Didcot OX11 0QX, UK*

[e] *Joint Institute for Nuclear Research, Dubna, Head Post Office, P.O. Box 79, SU-101 000 Moscow, USSR*

[f] *CERN, CH-1211 Geneva 23, Switzerland*

[g] *Instituto de Fisica Corpuscular (IFIC), Centro Mixto Universidad de Valencia–CSIC,*
Avda. Dr. Moliner 50, E-46100 Burjassot (Valencia), Spain

[h] *Department of Physics, University of Lund, Sölvegatan 14, S-223 63 Lund, Sweden*

[i] *Department of Physics, University of Bergen, Allégaten 55, N-5007 Bergen, Norway*

[j]   *Physics Laboratory, University of Athens, Solonos Street 104, GR-10680 Athens, Greece*

[k]   *Institut für Experimentelle Kernphysik, Universität Karlsruhe, Postfach 6980, D-7500 Karlsruhe 1, FRG*

[ℓ]   *Institute of Physics, University of Stockholm, Vanadisvägen 9, S-113 46 Stockholm, Sweden*

[m]   *Facultad de Ciencias, Universidad de Santander, av. de los Castros, E-39005 Santander, Spain*

[n]   *Laboratoire de l'Accélérateur Linéaire, Université de Paris-Sud, Bâtiment 200, F-91405 Orsay, France*

[o]   *Dipartimento di Fisica, Università di Trieste and INFN, Via A. Valerio 2, I-34127 Trieste, Italy*
     and Istituto di Fisica, Università di Udine, I-33100 Udine, Italy

[p]   *Istituto Superiore di Sanità, Istituto Nazionale di Fisica Nucleare (INFN), Viale Regina Elena 299, I-00161 Rome, Italy*
     and Dipartimento di Fisica, Università di Roma II and INFN, Tor Vergata, I-00173 Rome, Italy

[q]   *Nuclear Physics Laboratory, University of Oxford, Keble Road, Oxford OX1 3RH, UK*

[r]   *LPNHE, Universités Paris VI et VII, Tour 33 (RdC), 4 place Jussieu, F-75230 Paris Cedex 05, France*

[s]   *Fachbereich Physik, University of Wuppertal, Postfach 100 127, D-5600 Wuppertal 1, FRG*

[t]   *Laboratoire de Physique Corpusculaire, Collège de France, 11 place M. Berthelot, F-75231 Paris Cedex 5, France*

[u]   *Institute for High Energy Physics, Serpukhov, P.O. Box 35, SU-142 284 Protvino (Moscow Region), USSR*

[v]   *Greek Atomic Energy Commission, Nuclear Research Centre Demokritos, P.O. Box 60228, GR-15310 Aghia Paraskevi, Greece*

[w]   *Division des Hautes Energies, CRN–Groupe DELPHI, B.P. 20 CRO, F-67037 Strasbourg Cedex, France*

[x]   *Physics Department, Universitaire Instelling Antwerpen, Universiteitsplein 1, B-2610 Wilrijk, Belgium*
     and IIHE, ULB–VUB, Pleinlaan 2, B-1050 Brussels, Belgium
     and Service de Physique des Particules Elémentaires, Faculté des Sciences, Université de l'Etat Mons,
     Av. Maistriau 19, B-7000 Mons, Belgium

[y]   *Department of Physics, University of Liverpool, P.O. Box 147, Liverpool L69 3BX, UK*

[z]   *Dipartimento di Fisica Sperimentale, Università di Torino and INFN, Via P. Giuria 1, I-10125 Turin, Italy*

[α]   *Dipartimento di Fisica, Università di Bologna and INFN, Via Irnerio 46, I-40126 Bologna, Italy*

[β]   *NIKHEF-H, Postbus 41882, NL-1009 DB Amsterdam, The Netherlands*

[γ]   *Department of Radiation Sciences, University of Uppsala, P.O. Box 535, S-751 21 Uppsala, Sweden*

[δ]   *Dipartimento di Fisica, Università di Genova and INFN, Via Dodecaneso 33, I-16146 Genoa, Italy*

[ε]   *Department of High Energy Physics, University of Helsinki, Siltavuorenpenger 20 C, SF-00170 Helsinki 17, Finland*

[ζ]   *Physics Department, University of Oslo, Blindern, N-1000 Oslo 3, Norway*

[η]   *Dipartimento di Fisica, Università di Milano and INFN, Via Celoria 16, I-20133 Milan, Italy*

[θ]   *Dipartimento di Fisica, Università di Padova and INFN, Via Marzolo 8, I-35131 Padua, Italy*

[κ]   *Ames Laboratory and Department of Physics, Iowa State University, Ames IA 50011, USA*

[λ]   *Niels Bohr Institute, Blegdamsvej 17, DK-2100 Copenhagen Ø, Denmark*

[μ]   *Institute for Nuclear Studies, and University of Warsaw, Ul. Hoża 69, PL-00681 Warsaw, Poland*

[ξ]   *Physics Department, National Technical University, Zografou Campus, GR-15773 Athens, Greece*

[π]   *High Energy Physics Laboratory, Institute of Nuclear Physics, Ul. Kawiory 26 a, PL-30055 Cracow 30, Poland*

A search has been made for pairs of scalar quarks (squarks) produced in e^+e^- annihilations at LEP ($\sqrt{s} \simeq M_{Z^0}$), and decaying into a standard quark and a neutral, non-interacting, stable, massive particle (the lightest supersymmetric particle, LSP). The search has been conducted for differences in the mass of the squark and LSP of 2 GeV/c^2 and above. Up squarks with masses below 42 GeV/c^2 and down squarks below 43 GeV/c^2 were excluded. Six squark flavours degenerate in mass were excluded below 45 GeV/c^2.

1. Introduction

A large number of high energy e^+e^- annihilations have been recorded during the 1989 running period of LEP, the CERN electron–positron collider. Novel strategies that use the large statistics around the Z^0 resonance and rely on the clean machine conditions can be applied in searching for new phenomena.

This paper reports a search, using the DELPHI detector, for new heavy unstable charged particles which are pair produced in Z^0 decays, and decay immediately producing a neutral and non-interacting stable particle together with a standard quark. Decays of this type are to be expected in some theories beyond the standard model. In particular, supersymmetric models predict reactions of the type

$$e^+e^- \to Z^0 \to q\tilde{\bar{q}} \to \tilde{\chi}^0 q \tilde{\chi}^0 \bar{q} \,, \tag{1}$$

where the scalar supersymmetric partners $\tilde{q}$ and $\tilde{\bar{q}}$ of the quark and antiquark decay into the undetected lightest supersymmetric particle (LSP) $\tilde{\chi}^0$ and a quark q. Previous searches for these types of processes were based on the signature of a momentum imbalance appearing either as acollinear jets or as events with large missing transverse momentum [1–5]. Such approaches require a large difference between the mass of the charged decaying particle and the mass of the neutral invisible particle. In the case of a *heavy* invisible object, close in mass to the decaying particle, the experimental signature changes from a clearly distinguishable acollinear jet topology to events of small visible energy. At hadron colliders these events have low trigger efficiencies and high backgrounds due to soft processes. At e^+e^- colliders they are contaminated by two-photon interactions and machine backgrounds.

The present search was based on two different analyses. The *first* one applies to heavy invisible objects and is new. It utilises e^+e^- annihilations at center-of-mass energies around the Z^0 boson mass. The cross section of the new process is expected to follow the standard line shape of the Z^0 boson and, thus, to exceed on the peak the cross section due to s-channel photon exchange by several orders of magnitude. Data points at center-of-mass energies around the Z^0 pole are a direct experimental check of the estimates for the backgrounds which are decoupled from the Z^0. Hence the rates of these background events may be reliably determined. The *second* analysis which follows previous works [1,2], is based on searching for acollinear jets and puts limits for LSP masses less than about half of the squark mass. Most of the paper is devoted to an explanation of the new approach applied in the first analysis.

The squarks $\tilde{q}$ and $\tilde{\bar{q}}$ of eq. (1) couple to the Z^0 analogously to the corresponding fermionic quark fields and the expected cross sections are calculable for each flavour and helicity [6]. In case of low squark masses, the cross sections are the level of 3 nb for single flavours and they can contribute to the hadronic or to the invisible width of the Z^0 (depending on the mass of the LSP). The phase space factor $\beta^3 = (1 - 4M_{\tilde{q}}^2/s)^{3/2}$ affects the rates over a wide portion of the kinematically accessible region.
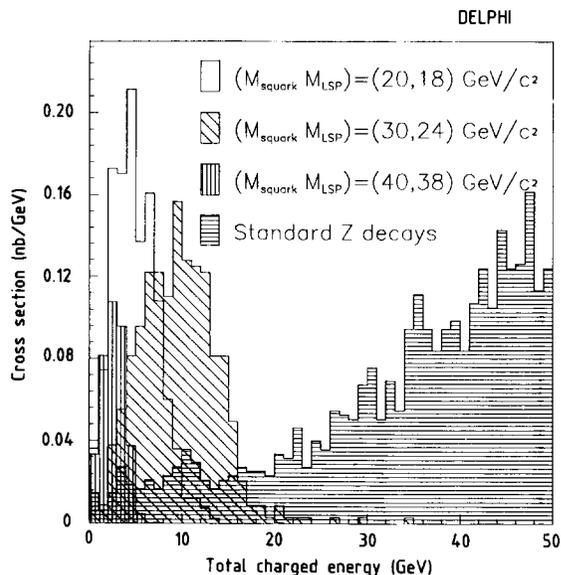
Fig. 1. The distributions of total charged visible energy in the final state of squark pair production for various squark and LSP masses.

In both analyses presented here, each squark was assumed to decay immediately with a 100% branching ratio into a LSP (heavy gluino assumed) and a quark. Only mass differences between the squark and the LSP above 2 GeV were investigated, since closer masses lead to theoretical uncertainties in the multiplicities of the fragmentation of low energy quark–antiquark systems. Some characteristics of the expected signal are shown in fig. 1 in which the distributions of the total charged energy are plotted for three combinations of the masses of the scalar quarks and the heavy LSP. In the first analysis the search was concentrated on events having a total charged energy smaller than 20 GeV whereas in case of LSP masses less than half of the squark mass, the total charged energy is well within the distribution from the standard quarks and events with visible energy larger than 15 GeV were considered.

2. The detector and trigger arrangement

The components of DELPHI [7] relevant for this work are the Time Projection Chamber (TPC), the Inner and the Outer Detectors (ID, OD), and the Small Angle Tagger (SAT).

The ID is a cylindrical drift chamber covering the polar angle range $30°–150°$. It contains five trigger layers giving information about the cylindrical $r\phi$ and longitudinal z coordinates at the radius of 22 cm around the beam axis. The jet chamber section providing the $r\phi$ coordinates of 24 points. The TPC is a cylinder with an inner radius of 30 cm, outer radius of 122 cm and with anode wires at a distance of 134 cm from the central high plane at $a = 0$. The TPC records 16 space points (for polar angles of $40–140°$), z-coordinates derived from the drift time onto the wires and $r\phi$ coordinates from the circular pad rows behind the anode wires. At least six space points are registered down to polar angles of $24°$. The OD is a cylindrical tracking device consisting of 24 aluminium drift tube assemblies in five layers at a radius of 198–208 cm. It provides five accurate $r\phi$ space points and three fast z coordinates per track at polar angles between $50°$ and $130°$ and contributed also to the track trigger. The SAT calorimeters cover polar angles of 43–135 mrad in the beam directions. They consist of scintillating fibres embedded in a lead absorber and they measure the integrated luminosity by monitoring the rate of small angle Bhabha scattering. Details of the luminosity measurement are given in ref. [8].

The component of the DELPHI trigger that is most important for this analysis is the barrel track trigger consisting of the coincidence of back to back OD quadrants with any signal from the ID trigger layers. The information about all the trigger components was included in the data on an event-to-event basis, and the efficiency of this particular trigger could be measured by using the redundancy of the independent barrel trigger information from the scintillator layer behind the first 5 radiation lengths of the barrel electromagnetic calorimeter combined with the 172 time of flight counters outside the solenoid. Fig. 2 shows the trigger efficiency as a function of the visible charged energy calculated from the data.
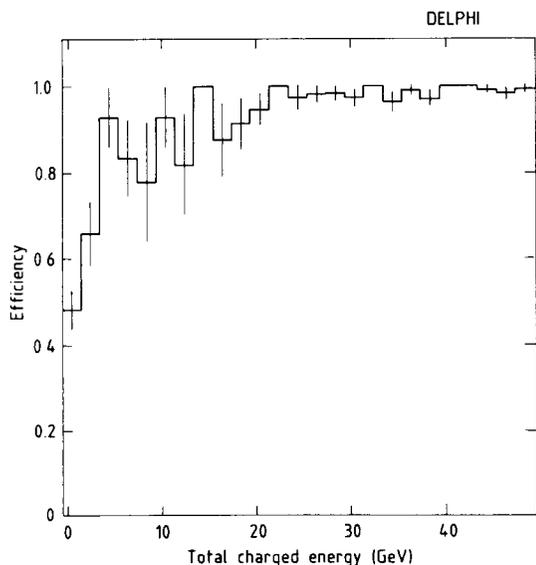
3. Event selection for heavy LSPs

Events used in this analysis contain at least one reconstructed charged track with a momentum larger than 0.5 GeV/c, a radial impact parameter less than 15 cm and a longitudinal distance z from the interaction point less than 30 cm. These selection criteria were chosen to include events to measure the machine backgrounds, as discussed later. The detector conditions were checked for the detector parts which were necessary for the reconstruction and the trigger. After this run selection 13 500 events remained, corresponding to an integrated luminosity of 330 nb^{-1} divided into ten samples at center-of-mass energies between 88.28 and 95.04 GeV.

In each event, the average impact distance in the z-direction, $\hat{z}$, and its variance, $\sigma(z)$, were calculated for the selected charged particle tracks.

The candidates were selected by requiring

(1) a total visible charged energy less than 20 GeV,

(2) more than two charged particles (this criterion rejected cosmic triggers, beam–halo tracks, and leptonic Z^0 decays, including a large fraction of the tau pairs, but had a high efficiency for signal events, because the average charged multiplicity in them is always larger than five,)

(3) $|\hat{z}| < 4$ cm (to reject events that are not at the expected interaction point),

(4) $\sigma(z) < 6$ cm (to reject events with an ill defined vertex),

(5) $|\cos\theta_{\text{thrust}}| < 0.8$, where θ_{thrust} is the polar angle of the thrust axis with respect to the beam (to reject most two-photon interactions),

DELPHI

Fig. 2. Efficiency of the DELPHI barrel track trigger used for this analysis as a function of the total visible charged energy.

(6) all tracks to have at angles greater than 25° to the beam axis (to veto events oriented very close to the beam direction),

(7) energy in the SAT smaller than 4 GeV (to veto two photon candidates and machine backgrounds).

After the selections the sample contained 284 events. It was checked by scanning that the general features of the events were those expected from a combination of two-photon events, Z^0 decays with low reconstructed charged energy and events due to machine backgrounds. Most of the off momentum tracks and the beam–gas or beam–wall interactions were rejected by the vertex criteria described above. The reference interval $5 < |\hat{z}| < 30$ cm was used to estimate the remaining beam associated background and its uncertainty. The 390 events in this interval were found to be uniformly distributed in the variable $\hat{z}$ within statistics. By extrapolating the event density to the vertex interval $|\hat{z}| < 4$ cm, a background of 62 ± 3 (stat.) events was estimated. The background rate turned out to be stable from machine fill to machine fill within the relatively poor statistics (often less than ten events per fill); to take into account possible variations, a 30% systematic

error was added in quadrature with the statistical error. This background was subtracted from the 284 selected events in the subsequent analysis. The number of selected events at each energy was normalized to the SAT measured luminosity to give the measured cross sections which are presented as a function of the center-of-mass energy in fig. 3.

The data of fig. 3 are taken to be the sum of a resonance-shaped contribution due to remaining Z^0 decays and a slowly energy dependent contribution due to the two photon events, that satisfy the selection criteria.

4. Expected signal and search limits in the case of a heavy LSP

A high statistics sample of Monte Carlo events was generated with first-order radiative corrections, quark fragmentation according to the Lund 6.3 parton shower model [9] and with the detailed simulation of the detector (ref. [10] shows the general properties of the hadronic Z^0 decays). This was used to estimate the contribution from standard hadronic Z^0 decays (reconstructed only partially due to either a very forward–backward event axis or high neutral content), and from decays into $\tau\bar{\tau}$ pairs. The result
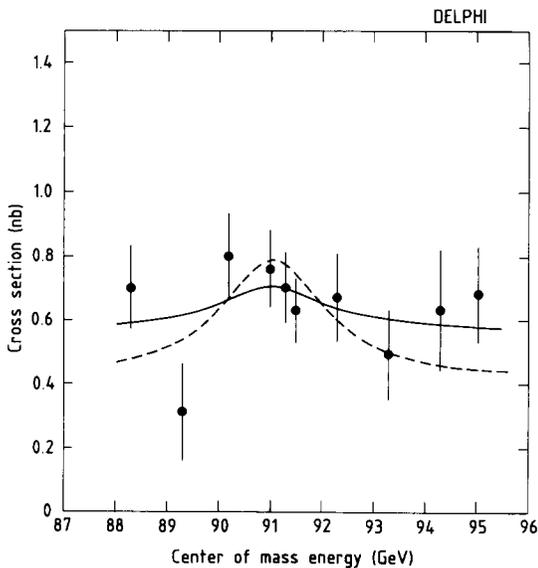
Fig. 3. Measured cross sections (corrected for the machine background) of events satisfying the selection criteria as a function of the center-of-mass-energy. The solid curve is the result of a two-parameter fit to a Z^0 line shape plus a constant term both with a free normalization. The dashed curve corresponds to the 95% CL upper limit.
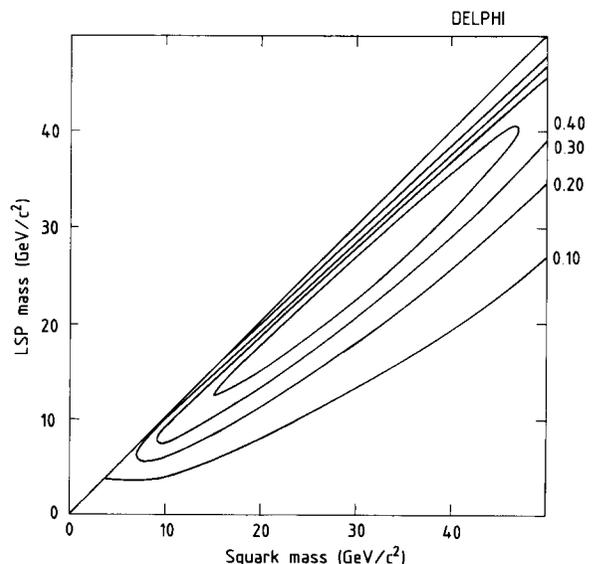
Fig. 4. Combined trigger and the selection efficiencies as a function of the squark mass and the LSP mass.
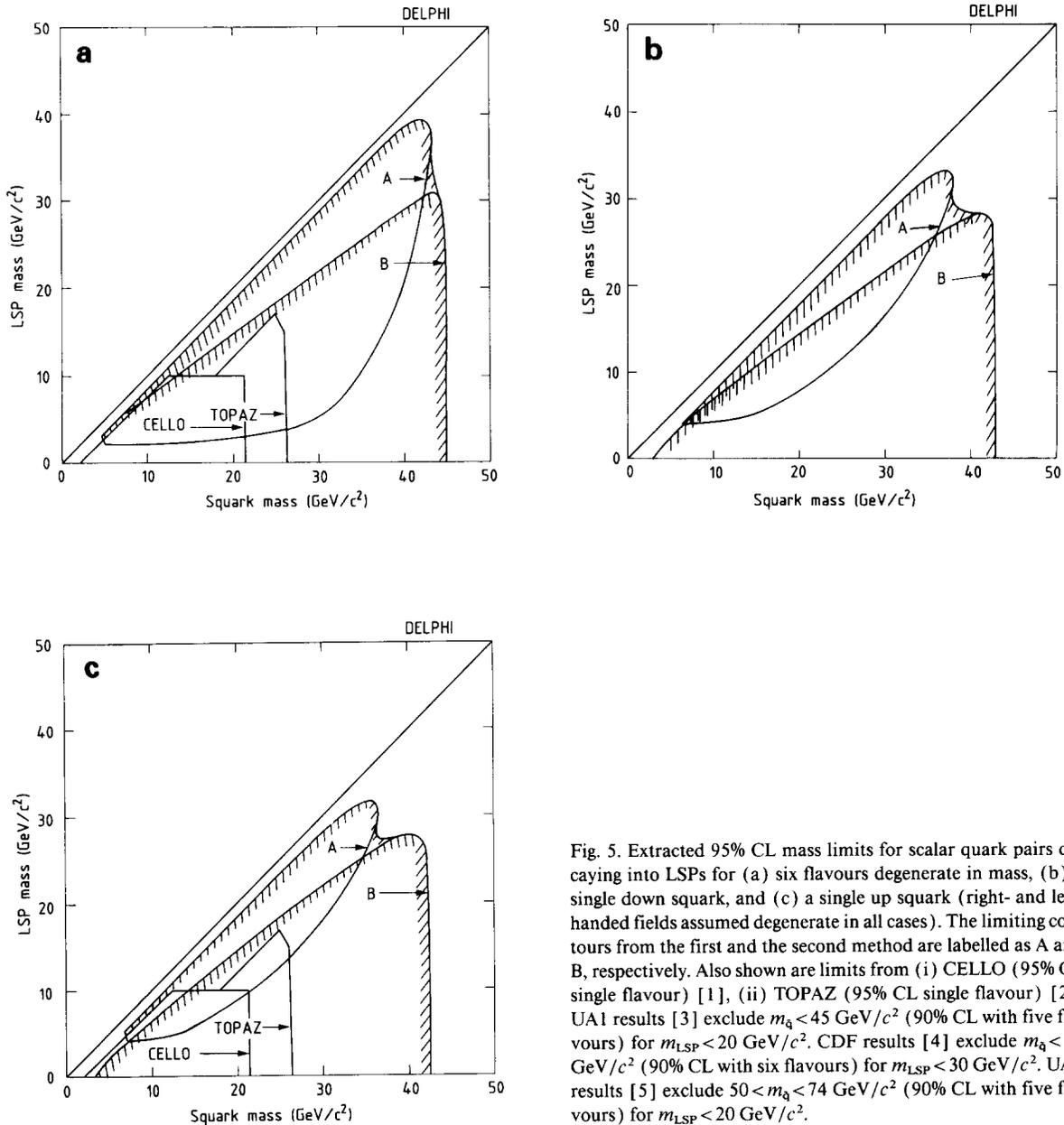
Fig. 5. Extracted 95% CL mass limits for scalar quark pairs decaying into LSPs for (a) six flavours degenerate in mass, (b) a single down squark, and (c) a single up squark (right- and left-handed fields assumed degenerate in all cases). The limiting contours from the first and the second method are labelled as A and B, respectively. Also shown are limits from (i) CELLO (95% CL single flavour) [1], (ii) TOPAZ (95% CL single flavour) [2]. UA1 results [3] exclude $m_{\tilde{q}} < 45$ GeV/c^2 (90% CL with five flavours) for $m_{LSP} < 20$ GeV/c^2. CDF results [4] exclude $m_{\tilde{q}} < 74$ GeV/c^2 (90% CL with six flavours) for $m_{LSP} < 30$ GeV/c^2. UA2 results [5] exclude $50 < m_{\tilde{q}} < 74$ GeV/c^2 (90% CL with five flavours) for $m_{LSP} < 20$ GeV/c^2.

was that $(0.75 \pm 0.25)\%$ of the standard Z^0 decays satisfy the selection criteria. The 0.25% systematic error was mainly due to uncertainties in the angular dependence of the trigger efficiency. The dependence of the tails of the charged energy distribution on the fragmentation model was investigated by comparing the α_s^2 matrix element Monte Carlo model with string fragmentation in Lund 6.3 and found to be negligi-

ble. These remaining Z^0's were assumed to be distributed according to the line shape and were normalised to the peak cross section measured in ref. [8]. Their contribution at the peak is equal to 0.23 ± 0.07 nb.

The measured cross section for all Z^0 associated processes was estimated by fitting to fig. 3 a Z^0 line shape [8] with a free normalization (representing the

remaining standard Z^0 plus possible nonstandard Z^0 decays) plus a constant term (representing the two-photon contribution). The fit had $\chi^2/\mathrm{DOF}=7.9/8$ (fig. 3). The expected background due to the standard Z^0 decays as estimated above was then subtracted from the result. The remaining nonstandard signal associated with the Z^0, for example due to process (1) was (-0.09 ± 0.14) nb on the peak. This corresponds to -20 ± 32 events integrated over the whole energy interval. The remaining constant background was 0.56 ± 0.09 nb. The upper limit for a physical, i.e. positive cross section, associated to nonstandard Z^0 decays was determined by excluding 95% of the probability density (gaussian) in the region of positive cross sections (ref. [11]). The limit was 0.23 nb, corresponding to 52 events. This number of events was used for deriving the search limits reported below.

The expected rate of the signal events depends on their production cross section, trigger efficiency and selection efficiency. The trigger and selection efficiencies were studied at various mass values by passing Monte Carlo samples through the same analysis chain as the real data. The trigger part of the simulation was cross checked against real data by comparing the simulation results with the trigger efficiency extracted from real events of a similar topology. The selection efficiency was found to vary from 34% to 56% as the mass difference between the squark and the LSP varied from 2 GeV to 6 GeV. For larger mass differences the efficiency decreases again since those events have more than 20 GeV of visible charged energy. The combined efficiency was parametrized as shown in fig. 4 and is known with an uncertainty of about 5%.

The 95% confidence level search limits for six degenerate flavours, for a single flavour downtype and for a single flavour uptype from this method are shown labelled as A in figs. 5a, 5b and 5c, respectively.

5. Analysis and limits for light LSP

In the second analysis, which used a sample corresponding to 9300 hadronic Z^0 decays, two-jet events were selected using the jet clusterization algorithm LUCLUS [9]. The acoplanarity angle α_{xy} was calculated as the angle between the two jets projected on the plane perpendicular to the beam axis. The candidates were selected with the following criteria:

(1) total visible charged energy larger than 15 GeV,

(2) more than five charged particles,

(3) $|\hat{z}|<4$ cm,

(4) $\sigma(z)<6$ cm,

(5) $|\cos\theta_{\mathrm{thrust}}|<0.7$,

(6) $\alpha_{xy}\leqslant135°$.

The first criterium was chosen in order to complement with some coverage the selection of section 3.

After the selection the sample contained 31 candidates. For estimating the expected background from standard Z^0 decays, the Monte Carlo events described in section 4 were used. It was found that 0.37% of the simulated standard hadronic Z^0 decays satisfied the selection criteria, which corresponds to 34 ± 4 (stat.) events in the selected sample. The systematic error was estimated to be 10% by comparing the distributions of the Monte Carlo events (with the parton shower fragmentation as well as with the string fragmentation) and the data in the variable $\alpha_{x,y}$. The background was subtracted from the number of candidate events, and a 5% systematic error in the normalization was added in quadrature with the other errors. The result was -3 ± 7.5 events. The upper limit of 13 for the number of signal events satisfying the selection criteria was determined by excluding 95% of the positive gaussian probability density.

The detection efficiency for the squark signal was parametrized analogously to fig. 4, being typically 25% for masses of the LSP up to half of the squark mass and for the squark masses larger than about 20 GeV/c^2. It was assumed to be known with about 5% uncertainty.

The 95% confidence level search limits based on this search are shown in fig. 5 labelled as B.

In conclusion, it is seen from fig. 5 that the combination of the two analyses exclude in the case of a LSP lighter than 20 GeV/c^2 three generations of squarks below 45 GeV/c^2, as single flavour downtype squark below 43 GeV/c^2 and a single flavour uptype squark below 42 GeV/c^2. For heavier LSPs (up to $m_{\tilde{q}}-2$ GeV/c^2) the limits extend to 44 GeV/c^2, 38 GeV/c^2 and 36 GeV/c^2, respectively. These results greatly improve the limits deduced from previous experiments, and are entirely new for the case of down type squarks.

After the completion of the present work a paper

by the Mark II Collaboration was received [12] where similar conclusions are reached.

Acknowledgement

References

[1] CELLO Collab., H.-J. Behrend et al., Z. Phys. C 35 (1987) 181.

[2] TOPAZ Collab., I. Adachi et al., Phys. Lett. B 218 (1989) 105.

[3] UA1 Collab., C. Albajar et al., Phys. Lett. B 198 (1987) 261.

[4] CDF Collab., F. Abe et al., Phys. Rev. Lett. 62 (1989) 1825.

[5] UA2 Collab., J. Alitti et al., Phys. Lett. B 235 (1990) 363.

[6] H. Haber and G. Kane, Phys. Rep. C 117 (1985) 75.

[7] DELPHI detector, to be submitted to Nucl. Instrum. Methods.

[8] DELPHI Collab., A precise measurement of the Z^0 resonance parameters through its hadronic decays, CERN preprint CERN-EP/90-32, submitted to Phys. Lett. B.

[9] T. Sjöstrand, Comput. Phys. Commun. 27 (1983) 243; 28 (1983) 229;
T. Sjöstrand and M. Bengtsson, Comput. Phys. Commun. 43 (1987) 367.

[10] DELPHI Collab., P. Aarnio et al., Phys. Lett. B 240 (1990) 271.

[11] Particle Data Group, G.P. Yost et al., Review of particle properties, Phys. Lett. B 204 (1988) 80–81.

[12] Mark II Collab., T. Barklow et al., SLAC preprint SLAC-PUB 5196 (March 1990).